



OPEN ACCESS

EDITED BY

Yimin Zhou,
Shenzhen Institutes of Advanced
Technology (CAS), China

REVIEWED BY

Srikanth Goud B.,
Anurag Group of Institutions, India
Yuewu Wang,
Guangxi University of Science and
Technology, China

*CORRESPONDENCE

Can Wang,
✉ xfcancan@163.com

SPECIALTY SECTION

This article was submitted to Smart Grids,
a section of the journal
Frontiers in Energy Research

RECEIVED 11 August 2022

ACCEPTED 29 December 2022

PUBLISHED 12 January 2023

CITATION

Chen R, Zhou L, Xiong C, Xu H, Zhang Z,
He X, Dong Q and Wang C (2023),
Islanding detection method for microgrids
based on CatBoost.
Front. Energy Res. 10:1016754.
doi: 10.3389/fenrg.2022.1016754

COPYRIGHT

© 2023 Chen, Zhou, Xiong, Xu, Zhang, He,
Dong and Wang. This is an open-access
article distributed under the terms of the
[Creative Commons Attribution License
\(CC BY\)](https://creativecommons.org/licenses/by/4.0/). The use, distribution or
reproduction in other forums is permitted,
provided the original author(s) and the
copyright owner(s) are credited and that
the original publication in this journal is
cited, in accordance with accepted
academic practice. No use, distribution or
reproduction is permitted which does not
comply with these terms.

Islanding detection method for microgrids based on CatBoost

Ran Chen¹, Li Zhou¹, Chuanyu Xiong¹, Hanping Xu¹,
Zhaoyang Zhang¹, Xuhui He^{2,3}, Qingguo Dong^{2,3} and Can Wang^{2,3*}

¹State Grid Hubei Economic Research Institute, Wuhan, China, ²Hubei Provincial Collaborative Innovation Center for New Energy Microgrid, China Three Gorges University, Yichang, China, ³College of Electrical Engineering and New Energy, China Three Gorges University, Yichang, China

The occurrence of unintentional islanding will seriously threaten the stable operation of a microgrid (MG). Therefore, detecting the islanding of an microgrid timely is an important premise to ensure the microgrid operates safely and stably. However, the problem of dead zone exists in the traditional islanding detection process because the threshold of various electrical feature quantities of the point of common coupling (PCC) cannot be determined effectively. To solve this problem, an islanding detection method based on CatBoost is proposed for an microgrid. The novelty of this method lies in two aspects: 1) To reduce the error brought by the electrical feature quantities with weak correlation in the process of islanding detection, an analysis method based on the Spearman correlation coefficient is used to extract the electrical feature quantities closely related to islanding detection. 2) To determine the threshold of the electrical feature quantities more accurately and reduce the dead zone of island detection, an integrated learning machine is used to dig out correlations between the electrical feature quantities and the operation of an microgrid. The performance of the proposed islanding detection method is verified based on the modified IEEE13-bus system. The results of the example verify that the proposed islanding detection can achieve higher detection accuracy in cases of grid-connected interference and line faults.

KEYWORDS

islanding detection, electrical quantities, CatBoost, microgrid, correlation

1 Introduction

As a new form of power supply that effectively integrates distributed generations (DGs), microgrids (MGs) can promote the development of DGs and improve the consumption capacity of the grid for DGs (Zhang et al., 2022). The power quality in MGs is the key to determining whether MGs can operate stably. When the power quality does not meet the requirements or the power supply is interrupted due to the failure of distribution networks, the DGs will continue to supply the load, thus forming an islanding state of the MGs (Wang et al., 2022a; Liu et al., 2022). After the occurrence of islanding, the DGs should take corresponding control measures to change their inverter control mode, and even implement the corresponding load shedding strategy when the power shortage is serious. Otherwise, the power shortage will lead to voltage and frequency instability in the islanding MG, and the power equipment will be damaged in serious cases (Davari et al., 2021; Wang et al., 2022b).

Effective islanding detection of MGs is key and prerequisite to preventing the delinking of islanding MGs during the process of islanding transition. Therefore, from a safety point of view, the MGs should have the ability of timely islanding detection. At present, the research on islanding detection technology is mainly divided into active islanding detection and passive islanding detection. In (Sivadas and Vasudevan, 2020), an active islanding detection method was proposed for an MG containing multiple inverters operating in parallel. This method

realizes accurate identification of islanding mode by constructing a predefined pattern with small periodic steps during the process of islanding detection. In (Gupta et al., 2015), an average absolute frequency deviation value based active islanding detection technique was proposed. This detection method can detect the occurrence of islanding and maintain the stable operation of systems under the condition of small frequency deviation. In (Murugesan et al., 2018), an active islanding detection method based on generator d-axis current disturbance was proposed. This active islanding detection method can quickly detect the occurrence of islanding while maintaining the stable operation of DGs. In (Wen et al., 2016), an impedance-based analysis of the active frequency drift (AFD) islanding detection method was proposed. In this method, the output impedance of the inverter is modeled and the frequency detection unit can accurately judge the occurrence of islanding according to the frequency drift of the inverter. The active islanding detection methods are mainly to inject a disturbance signal into the system and judge whether islanding occurs by using the change of electrical feature quantities caused by the disturbance signal. However, these methods can affect the power quality.

To avoid the impact of the islanding detection process on the power quality of MGs, the passive islanding detection method has been widely studied. In (Seyedi et al., 2021), a new method for islanding detection based on the combination of the rate of change of voltage (ROCOV) and the rate of change of active power (ROCOAP) was proposed. This method overcomes the disadvantage that the traditional passive islanding detection methods may fail when the power mismatch is close to zero. In (Makwana and Bhalja, 2019), an islanding detection method based on the modal component of the voltage signal was proposed. This method can quickly identify the occurrence of islanding under the condition of complete power balance in an MG. In (Bakhshi et al., 2018), an islanding detection method based on the chaos theory was proposed. This method takes the correction frequency at the point of common coupling (PCC) as the input signal of the forced Helmholtz oscillator and determines the threshold of the islanding detection index by using the chaotic motion of the forced Helmholtz oscillator and the obvious change of normal motion. In (Bakhshi-Jafarabadi et al., 2021), a two-level islanding detection method using the rate of change of output voltage and the change of active power output was proposed. This method can achieve independent determination of the threshold and does not adversely affect the output power quality of DGs. However, the passive islanding detection methods rely on the change of the electrical feature quantities of the inverter when the islanding occurs, and there are shortcomings such as detection blind area and low detection accuracy. In addition, the large uncertainty and power volatility of DGs operation will lead to the failure of the passive islanding detection methods in some scenarios.

In recent years, the application of machine learning algorithms in islanding detection has been widely studied. The application of machine learning algorithms can improve the shortcomings of traditional active and passive islanding detection methods, and improve the rationality and efficiency of islanding evaluation. In (Ezzat et al., 2021), a two-stage islanding detection method based on K-nearest neighbor (KNN) was proposed. This method can correctly identify the occurrence of islanding in the presence of noise and has the advantages of high recognition accuracy and short detection time. In (Baghaee et al., 2020), an islanding detection method for photovoltaic power plants based on a support

vector machine (SVM) was proposed. This method effectively solves the problem of indistinguishable islanding events and grid fault events in multiple complex scenario tests. In (Kermany et al., 2017), an islanding detection method for MGs with multiple connection points to smart grids was proposed. This method uses artificial neural networks (ANNs) to move the current and voltage measurement locations from the PCC to the distribution network side during the signal processing, thereby reducing the islanding detection time. In (Alshareef et al., 2014), a passive islanding method for DGs based on wavelet design and machine learning was proposed. This method uses the procrustes analysis method to determine the filtering coefficient of the designed wavelet and improves the adaptability of the machine learning algorithm in islanding detection. In (Özcanlı and Özcanlı, 2022), an islanding detection method based on long short-term memory (LSTM) was proposed. The islanding detection method achieves accurate detection of islanding without affecting the power quality and operation stability of the MG. However, the above islanding detection methods do not analyze the correlation between electrical feature quantities at the PCC and the islanding states. The selection of electrical feature quantities at the PCC is closely related to the islanding detection method. If the training samples of the islanding detection method contain irrelevant or weakly correlated electrical feature quantities, feature conflicts and key features will be underestimated, which will affect the accuracy of the islanding detection method.

To solve the above problems, this paper extracts electrical feature quantities with a strong correlation with islanding detection based on the Spearman correlation coefficient. In addition, to effectively determine the threshold of multiple electrical feature quantities and reduce the dead zone in the islanding detection process, an islanding detection method based on CatBoost is proposed for an MG in this paper. This method trains the islanding detection method in the dataset generated by islanding, grid-connected interference, and line fault by CatBoost. It learns to explore the correlation between multiple electrical feature quantities and the operating state of the MG, so as to determine the threshold of electrical feature quantities in the process of islanding detection and realize the accurate detection of islanding. The proposed method can effectively improve the defects of the traditional active and passive islanding detection methods, and improve the accuracy of the islanding detection methods.

The main contributions of this paper are as follows:

- 1) To reduce the interference of weak correlation electrical feature quantities on the islanding detection method, an islanding state feature extraction method based on the Spearman correlation coefficient is proposed in this paper. By analyzing the correlation between multiple electrical feature quantities and the operating states of an MG, this feature extraction method extracts the electrical feature quantities with a strong correlation with the islanding states. This method can reduce the errors caused by weakly correlated electrical feature quantities in the islanding detection method.
- 2) To determine the threshold of various electrical feature quantities and reduce the dead zone in the process of islanding detection, an islanding detection method based on CatBoost is proposed for an MG. As an ensemble learner, this method has strong performance in the multidimensional data processing. It can fully learn data sets and determine the threshold of electrical feature quantities to accurately detect islanding.

TABLE 1 Multiple electrical feature quantities at PCC.

Name	Symbol
Active power	P
Active power change rate	dP/dt
Frequency	f
Frequency change rate	df/dt
Voltage	U
Voltage change rate	dU/dt
Current	I
Current change rate	dI/dt
Total harmonic distortion of voltage	THD_U
Total harmonic distortion of current	THD_I

2 Feature extraction

The islanding detection method proposed in this paper is to judge whether the islanding occurs in the MG according to the electrical feature quantities at the PCC between the MG and the distribution network. The PCC can provide rich instantaneous electrical feature quantities information (Mlakić et al., 2019; Chaitanya et al., 2021). Table 1 shows the common electrical feature quantities that can be used in islanding detection at the PCC. The ideal electrical feature quantities applied to the islanding detection of the MG should be highly correlated with the operation states of the MG and can produce obvious changes before and after the islanding of the MG. At the same time, the ideal electrical feature quantities should be insensitive to faults and power quality disturbances in the MG. Therefore, it is necessary to analyze the correlation between multiple electrical feature quantities at the PCC and the operation states of the MG.

During islanding detection, the time and complexity of islanding detection will increase dramatically if all the electrical feature quantities in Table 1 are used as the criterion of islanding detection. In addition, the electrical feature quantities at the PCC contain much weak correlation information with islanding detection. The information will affect the judgment of the islanding detection method and bring errors in islanding detection. Therefore, it is necessary to extract the characteristic of relevant electrical feature quantities and dig out the effective information related to islanding detection. In this paper, the Spearman correlation coefficient is used to analyze the correlation between the electrical feature quantities at the PCC and the islanding states, and the electrical feature quantities with a large correlation with the islanding state are extracted. The extracted electrical feature quantities are used as the islanding detection index to improve the efficiency and accuracy of the islanding detection method.

The Spearman correlation coefficient can measure the correlation between two variables (Zhang et al., 2016; Jia et al., 2021). This method can be used to extract the key information for judging the islanding state of the MG, and enhance the mapping relationship between the electrical feature quantities at the PCC and the islanding judgment. The specific steps of the electrical feature quantities correlation analysis based on the Spearman correlation coefficient proposed in this paper are as follows:

Step 1: The electrical feature quantities data set x_i^k at the PCC and the data set y of the islanding state of the MGs are constructed, and the data set is expressed as

$$x_i^k = (x_1^k, x_2^k, \dots, x_{n-1}^k, x_n^k) \quad (1)$$

$$y = (y_1, y_2, \dots, y_{n-1}, y_n) (y_n \in \{0, 1\}) \quad (2)$$

where k is the k_{th} electrical feature quantities at the PCC and n is the total number of the electrical feature quantities.

Step 2: x_i^k and y in ascending or descending order are arranged, the sorted position r_i as the rank of x_i^k recorded and its corresponding rank sequence r is determined. Similarly, y is sorted and the rank sequence s of y_i is obtained.

Step 3: Each element of the sequence r and the sequence s is subtracted to obtain the rank difference sequence $d = (d_1, d_2, \dots, d_{n-1}, d_n)$, and d is brought into the calculation formula to obtain the Spearman correlation coefficient ρ . The Spearman correlation coefficient ρ is expressed as

$$\rho = 1 - \frac{6 \sum_{i=1}^n d_i^2}{n(n^2 - 1)} \quad (3)$$

where n is the sequence length of the variable.

The range of the Spearman correlation coefficient is $[-1, 1]$. A negative value means negative correlation, and a positive value means positive correlation. The greater the absolute value is, the greater the correlation is. The closer the value of the Spearman correlation coefficient ρ is to 0, the smaller the correlation between them is.

3 Proposed islanding detection method

3.1 CatBoost introduction

The traditional active and passive islanding detection methods need to manually set the threshold, and there is a certain detection dead zone. The disturbance signals injected by some traditional islanding detection methods will also adversely affect the power quality in the MG. The application of machine learning in islanding detection can improve the defects of traditional active and passive islanding detection methods. Machine learning avoids the manual setting of the thresholds in islanding detection, and can accurately detect the islanding state of an MG by learning various electrical feature quantities measured at the PCC and further determining the thresholds of electrical feature quantities.

The traditional single machine learning algorithms are prone to low precision in multi-feature data processing. The emergence of integrated machine learning algorithms avoids the defects of single machine learning algorithms. As a typical representative algorithm in the integrated machine learning algorithm, CatBoost is developed based on the GBDT framework. CatBoost has a good performance in processing categorical features, gradient deviation, and prediction offset, and can reduce the occurrence of overfitting, thereby improving the accuracy of the algorithm (Samat et al., 2021; Samat et al., 2022).

CatBoost is composed of Categorical and Boosting. By training the weighted training set, several weak learners are formed, and the weight

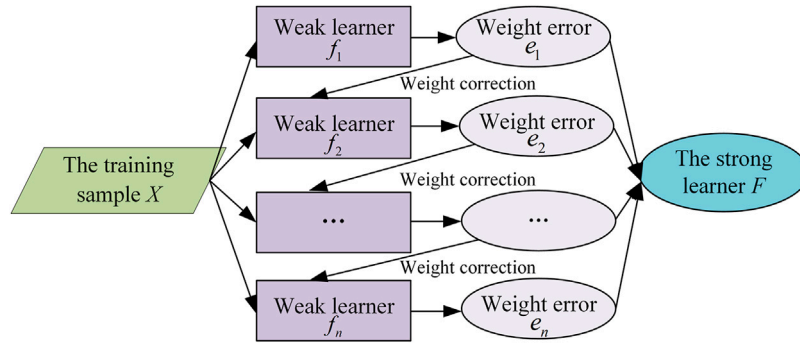


FIGURE 1
Diagram of CatBoost structure.

errors are fed back for weight correction. Finally, a strong learner based on several learners is formed. Its structure diagram is shown in Figure 1.

It is assumed that the observation data set $S = \{(X_1, Y_1), (X_2, Y_2), \dots, (X_n, Y_n)\}$, where $X_i = \{x_i^1, x_i^2, \dots, x_i^m\}$ is the m -dimension vector containing numerical and categorical features, and Y_i is the marker value.

First, the CatBoost model binaries all numeric features: the tree of oblivious is used as the base predictor to binarize floating-point features, statistics, and one-hot coding.

Second, categorical features are marked as numerical values:

- (1) The observed values are randomly arranged to generate multiple random sequences.
- (2) For a certain sequence, the average marker values of the training data set are used to mark the categorical features:

$$x_i^k = \frac{\sum_{j=1}^n [x_j^k = x_i^k] \cdot Y_j}{\sum_{j=1}^n [x_j^k = x_i^k]} \quad (4)$$

where, if $x_j^k = x_i^k$, then $[x_j^k = x_i^k] = 1$; otherwise, it is 0. The same values of the categorical features are placed before the given values of the sequences.

- (3) It is assumed that $\theta = (\theta_1, \theta_2, \dots, \theta_n)$, the values of the categorical features are converted to the numerical values:

$$x_{\theta^p}^k = \frac{\sum_{j=1}^{p-1} [x_{\theta^j}^k = x_{\theta^p}^k] Y_{\theta^j} + a \cdot P}{\sum_{j=1}^{p-1} [x_{\theta^j}^k = x_{\theta^p}^k] + a} \quad (5)$$

where, prior value P and parameter $a (a > 0)$ are added, namely prior weight, which is helpful to reduce the noise of the low frequency category.

Finally, when dealing with feature combinations, CatBoost combines with a greedy strategy: 1) The first split of the tree does not combine at all; 2) The second split of the tree combines all the existing combination and classification features in the current tree and all the classification features in the data set. At the same time, the new combined categorical features are converted into numerical features; 3) All the splits selected in the tree are considered categorical features

with two values, and are used to generate a combination of numerical features and categorical features.

In the process of overcoming gradient bias, CatBoost constructs a tree in two stages: 1) CatBoost selects the tree structure and calculates the value of leaf nodes after the tree structure is fixed; 2) CatBoost enumerates different splitting methods, and scores the obtained tree by calculating the values of leaf nodes, so as to select the best segmentation. The values of leaf nodes in the two stages are calculated using the approximation of the gradient.

CatBoost synchronizes training data sets and processing categorical features, which greatly improves the efficiency of feature processing. The algorithm for calculating leaf nodes can effectively avoid overfitting and reduce the need for hyperparameter tuning, which makes the model more universal. At the same time, CatBoost binaries floating-point features, statistics and one-hot encoded features, and achieves binarization of model output in the scoring process.

3.2 Islanding detection process based on CatBoost

The islanding detection method based on CatBoost in this paper mainly includes sample construction, weak learner generation, loss function gradient determination, and final strong learner generation. The specific contents are as follows:

- 1) Sample set construction

Firstly, data set $\{(x_1, y_1), (x_2, y_2), \dots, (x_{n-1}, y_{n-1}), (x_n, y_n)\}$ is obtained by constructing n samples from the electrical feature quantities at the PCC, where $x_i = (x_i^1, x_i^2, \dots, x_i^{k-1}, x_i^k)$ ($i = 1, 2, \dots, n$) is the i th sample formed by the electrical feature quantities at the PCC, and k is the dimension of the i th sample. $y_i (i = 1, 2, \dots, n) (y_i \in \{0, 1\})$ is the islanding state label corresponding to the i th sample, where 0 represents the grid-connected state and 1 represents the islanding state.

- 2) Generation of weak learner

After constructing the sample set, the initial weak learner f_1 is constructed by constructing the classification and regression trees (CART), and the weight error e_i is fed back to update the weight. Finally, a strong learner F based on several learners is formed. Before

generating F , in the total L rounds iterative process, the output of the previous round of the l th ($l = 2, 3, \dots, L$) generates the strong learner F_{l-1} , and the loss function is obtained according to F_{l-1} , and the learning results to describe the difference between the predicted value and the real value of the sample in the islanding detection process. The purpose of iterative learning in the l round is to find a weak learner f_l of the decision tree model to minimize the iterative loss function in this round. f_l is expressed as

$$f_l = \operatorname{argmin} \sum_{i=1}^n L(y_i, F_{l-1}(x_i) + f_l(x_i)) \quad (6)$$

where $f_l(x_i)$ is the output value of the weak learner f_l when the input is x_i , and $L(y_i, F_{l-1}(x_i))$ is the loss function of the strong learner F_{l-1} .

3) Loss function gradient determination

The negative gradient of the loss function for the i th sample in the l round is:

$$g_l^i = -\frac{\partial L(y_i, f_{l-1}(x_i))}{\partial f_{l-1}(x_i)} \quad (7)$$

For each sample input x_i , the corresponding loss function negative gradient g_l^i can be obtained, and then the weak learner of this round can be fitted by set $\{(x_1, g_l^1), (x_2, g_l^2), \dots, (x_{n-1}, g_l^{n-1}), (x_n, g_l^n)\}$. To make g_l^i unbiased for the weak learner and avoid the prediction offset existing in the generation of the strong learner, the proposed islanding detection method adopts the gradient estimation method of the sorting boosting algorithm. For each sample x_i , a separate learning model M_i is obtained by training with samples other than x_i , and the negative gradient of the loss function on x_i is calculated by using this learning model M_i . This method avoids the gradient deviation in the gradient calculation process and realizes the unbiased estimation of the gradient.

4) Generation of the final strong learner

The proposed islanding detection method uses a symmetric tree as the basic predictor. In this type of tree, the same partitioning criterion is used on the entire level of the tree. This tree is balanced and less prone to overfitting. In a symmetric tree, the index of each leaf node can be encoded as a binary vector of length equal to the depth of the tree, and the evaluation result is calculated by using binary features during prediction. The strong learner formed after l rounds of iterations is $F_l(x)$, and its expression is expressed as

$$F_l(x) = F_{l-1}(x) + f_l \quad (8)$$

After the strong learner in the L rounds of iteration and the weight update based on the weight errors, the proposed islanding detection method can be obtained.

The electrical feature quantities at the PCC under various operation scenarios of an MG are taken as the input, and the islanding label of the MG is taken as the output. The flow chart of the proposed islanding detection method is shown in Figure 2, and the detailed steps of the islanding detection are as follows:

- 1) The hyperparameters of CatBoost and fault events are initialized.
- 2) The Spearman correlation coefficient analysis method is used to extract the islanding strong correlation electrical feature quantities at the PCC of the MG under fault events.

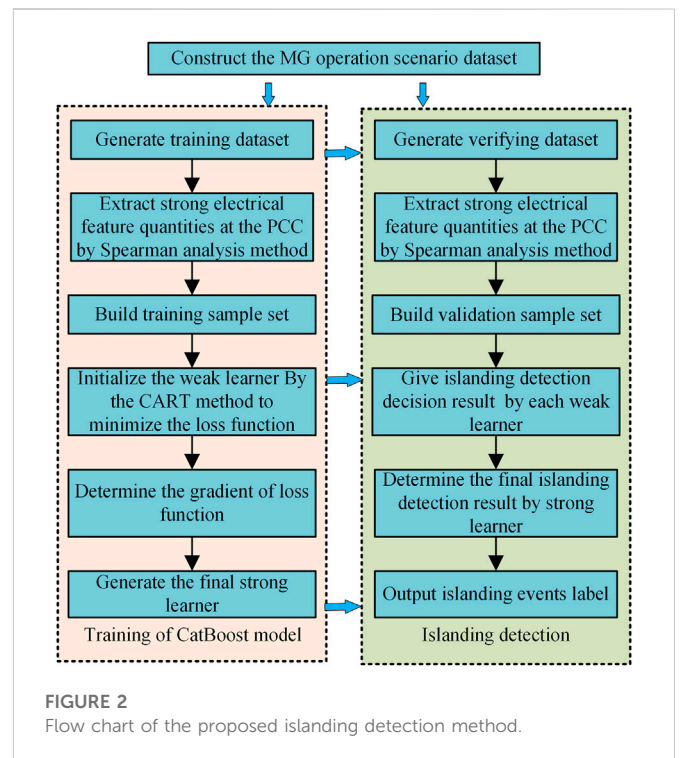


FIGURE 2 Flow chart of the proposed islanding detection method.

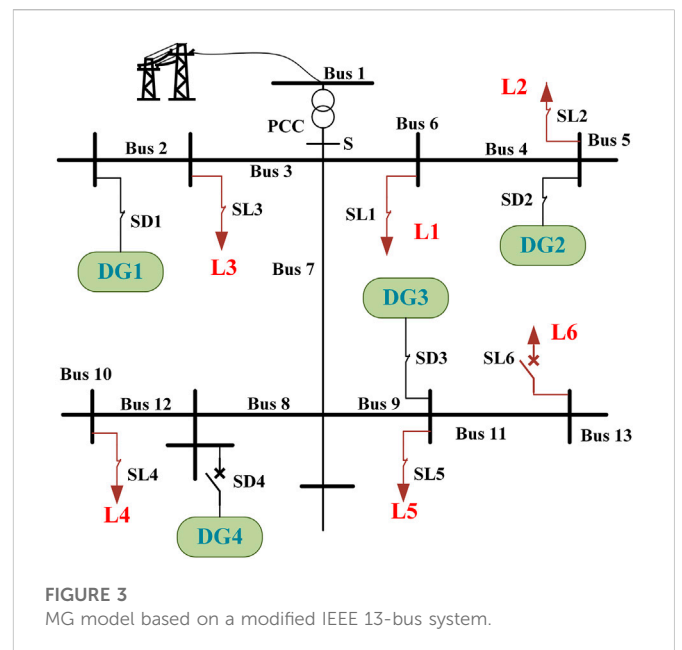


FIGURE 3 MG model based on a modified IEEE 13-bus system.

- 3) The data of islanding strong correlation electrical feature quantities at the PCC is input to the pre-trained CatBoost model.
- 4) Each weak learner in the CatBoost model gives its own islanding decision result of the MG.
- 5) The strong learner generated by the training of CatBoost model gets the final decision of islanding detection according to the weight of each weak learner.
- 6) The islanding event label is output.

TABLE 2 Data information of DGs and loads.

	Rate power/kW	Real time power/kW
DER1	30	30
DER2	40	40
DER3	50	50
DER4	60	60
L1	50	45
L2	60	57
L3	40	40
L4	50	50
L5	50	45
L6	30	30

4 Simulation studies and results

The setting of the samples can determine the learning result of the machine learning algorithm and then affect the islanding detection accuracy. To include the operation situations of MGs in grid-connected and islanded states as much as possible, a modified IEEE 13-bus system shown in Figure 3 is built based on MATLAB/Simulink in this paper. All tests are conducted on a computer equipped with Intel(R) Core(TM) i5-7500, which operates at 3.40 GHz and is equipped with 16 GB of running memory. The test system contains 4 DGs and 6 loads. In the system, the AC power grid is a three-phase power supply. The line voltage and DC bus voltage are 380 and 600 V respectively. The frequency is 50 Hz. The data information of DGs and loads are shown in Table 2. The parameter Settings of the CatBoost model are shown in Table 3.

To train and detect the proposed islanding detection method more comprehensively, and reduce the interference of different operation states of MGs on islanding detection, this paper comprehensively considers the switching of DGs and loads in the islanding scenario and the grid-connected scenario. At the same time, the short-circuit and open-circuit faults of transmission lines are also considered in the case of MG grid-connected mode. Various simulated events are shown in Table 4. In addition, to more comprehensively reflect the different

operating states of MGs, the power imbalance in the MG is considered on the basis of the above state settings (Faqhruldin et al., 2014).

This paper comprehensively considers the islanding events, grid-connected interference events, and line fault events shown in Table 3. In the range $[0, .7]$ of power imbalance degree in the MG, 15 groups are taken at an interval of .05, and a total of 330 groups of data are generated. This paper not only considers the situation of MGs as the power receiver but also considers the situation of MGs as the power supplier of the distribution network. Three groups of data in the value range $[-1, 0]$ are taken to generate a total of 66 groups of data. A total of 396 groups of data are generated under the two conditions.

4.1 Analysis of feature extraction results

In the constructed 396 sets of data, the Spearman correlation coefficient is used to analyse the correlation between the islanding state and the electrical feature quantities at the PCC. The Spearman correlation coefficient analysis results are shown in Figure 4.

According to the correlation strength classification criteria in Table 5, the absolute value $|\rho|$ of the Spearman correlation coefficient ρ is used to classify the correlation strength (Zhao et al., 2022). The correlation analysis results show that the frequency f of the electrical feature quantities, the frequency change rate df/dt , the voltage total harmonic distortion THD_U , the current total harmonic distortion THD_I , and the MGs operating state $|\rho|$ are greater than .8, and their correlation strength is “very strong.” The current change rate dI/dt and $|\rho|$ are greater than .7, and their correlation strength is “strong.” However, the active power P , the active power change rate dP/dt , the voltage U , the voltage change rate dU/dt , the current I , and $|\rho|$ are less than .6. The correlation between these electrical feature quantities and MG operating states is weak. In this paper, f , df/dt , dI/dt , THD_U , and THD_I are selected as the electrical feature quantities used in the islanding state detection method. The purpose is to select the electrical feature quantities that are strongly related to the MG operating states among the 10 electrical feature quantities, and avoid the use of many electrical feature quantities at the same time. According to the islanding detection standard IEEE Std. 1547, the detection time cannot exceed 2 s (Kermany et al., 2017). Considering the detection time and data input delay of the islanding detection method, an average value of the electrical feature quantities in 3 consecutive cycles is selected in this

TABLE 3 The parameters of CatBoost model.

Parameter	Parameter specification	Parameter values
Iterations	Maximum number of trees	100
Depth	The depth of the tree	5
Learning_rate	Learning rate	.1
Loss_function	Loss function	Logloss
Eta	Step of contraction	.5
Min_child_weight	Minimum weight sum of sample leaf nodes	5
Eval_metric	Prevent overfitting parameters	Accuracy
Calc_feature_importance	Prevent overfitting parameters	1
One_hot_max_size	Prevent overfitting parameters	1

TABLE 4 MG different state settings.

Simulate event	Event situations	Simulate events	Event situations
Islanding events	1. PCC disconnect	Grid-connected interferences	1. SD1, SL1, and SL2 disconnect
	2. PCC and SL1 disconnect		2. SD2, SL2, and SL3 disconnect
	3. PCC and SL2 disconnect		3. SD3, SL4, and SL5 disconnect
	4. PCC and SL3 disconnect		4. SD3 disconnect
	5. PCC and SL4 disconnect		5. SD1 and SD2 disconnect
	6. PCC and SL5 disconnect		6. SL1,SL2, and SL3 disconnect
	7. PCC and SD1 disconnect		7. Connect SD4
	8. PCC and SD2 disconnect		8. Connect SL6
	9. PCC and SD3 disconnect	Line faults	Single-phase/two-phase/three-phase short circuit

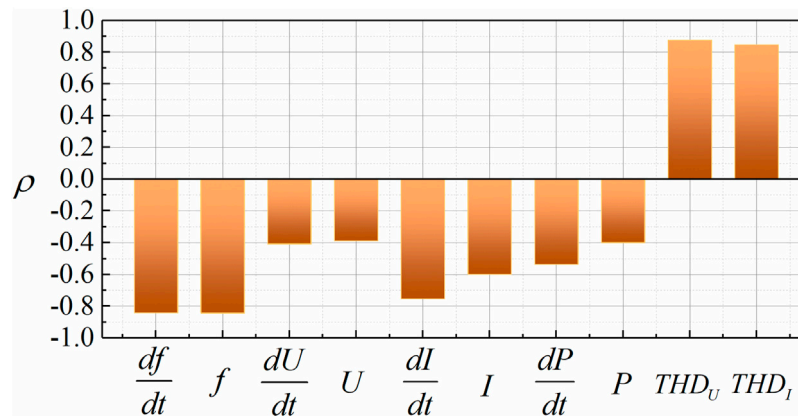


FIGURE 4 Spearman correlation coefficient between each electrical quantity and MGs state.

TABLE 5 Correlation strength classification.

The value ranges of $ \rho $	Correlation strength
[0.8, 1]	Very strong
[0.6, 0.8)	Strong
[0.4, 0.6)	Moderate
[0.2, 0.4)	Weak
[0, 0.2)	Very weak

paper after the islanding occurs when collecting the electrical feature quantities.

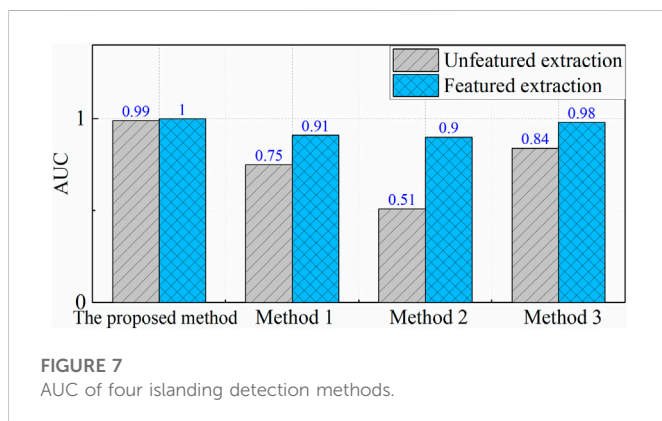
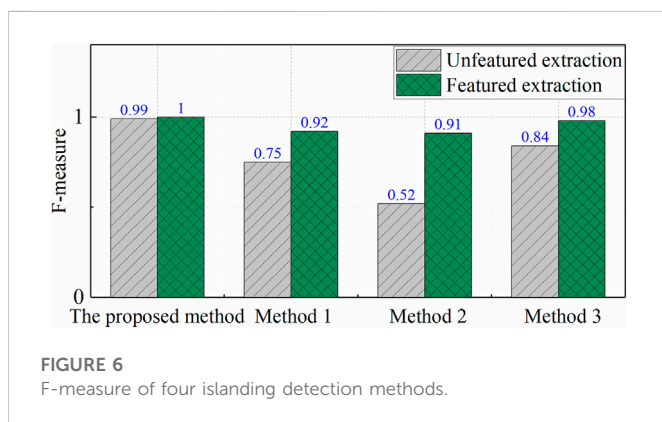
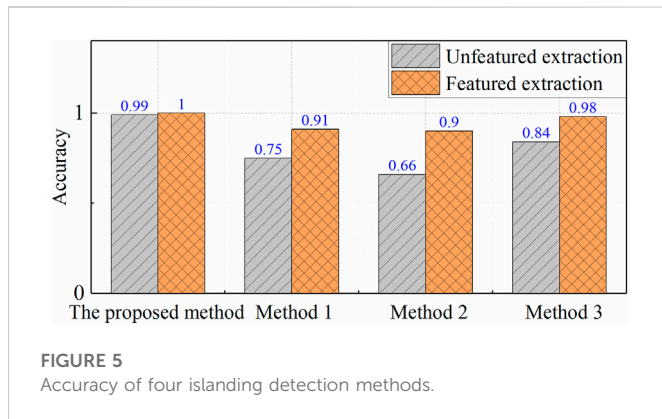
4.2 Result analysis of islanding detection method

In the cases of islanding events, grid-connected interference events and line faults are extracted to obtain electrical eigenvalues for islanding detection, which together with the islanding state

constitute the training samples of the islanding detection method. To verify the performance of the proposed islanding detection method based on CatBoost, this paper compares the proposed islanding detection method with three different islanding detection methods. Comparison method 1 is the islanding detection method based on K-nearest neighbor (KNN) (Ezzat et al., 2021), comparison method 2 is the islanding detection method based on a support vector machine (SVM) (Baghaee et al., 2020), and comparison method 3 is the islanding detection method based on artificial neural network (ANN) (Kermany et al., 2017). In addition, the accuracy, F-measure, and AUC value indicators are selected as the evaluation indicators of the islanding detection method (Xia et al., 2022). The values of accuracy, F-measure, and AUC represent the reliability and accuracy of the islanding detection method, and the closer the value is to 1, the higher the reliability of the islanding detection method.

4.3 Case 1: Analysis of the impact of feature extraction on islanding deflection method

To verify the reliability of the islanding detection method and the influence of feature extraction on the islanding detection method, a



comparative analysis of different detection methods is carried out in the two cases of feature extraction and no feature extraction in this paper. At the same time, to ensure that the sample proportions of islanding events and grid-connected interference events in the training set and validation set are consistent with the full set of samples, stratified proportional sampling is used to divide the total sample set into a sample set A and a sample set B according to the ratio of .7:3. The proposed islanding detection method, comparison method 1, comparison method 2, and comparison method 3 are trained by taking sample set A as the training sample set. Sample set B is used as the

verification sample to verify the performance of the islanding detection methods trained by sample set A. The accuracy, F-measure, and AUC values of the proposed islanding detection method, comparison method 1, 2, and 3 based on sample set B are shown in Figures 5–7.

When there is no feature extraction and the four islanding detection methods detect the islanding state based on 10 electrical feature quantities, the values of accuracy, F-measure, and AUC of the proposed method, comparison methods 1, 2, and 3 are shown in Figures 5–7, respectively. The accuracy, F-measure, and AUC values obtained by comparison method 1 are all below .8. These values obtained by comparison method 2 are all below .7, and the F-measure and AUC values are even around .5. These values obtained by comparison method 3 are all below .9. These values obtained by the proposed method all reach .99. When judging the islanding state based on 10 electrical feature quantities, the proposed islanding detection method is significantly better than comparison methods 1, 2, and 3. However, the accuracy, F-measure, and AUC values obtained by the four islanding detection methods do not reach 1, which shows that the four islanding detection methods fail to accurately judge the islanding state of the MGs without feature extraction.

After using the Spearman correlation coefficient to extract the characteristics of electrical feature quantities, five electrical feature quantities which have a strong correlation with the islanding state of the MG are extracted from the original 10 electrical feature quantities. By analyzing the islanding detection results before and after feature extraction, it can be concluded that the values of accuracy, F-measure, and AUC of comparison method 1 are increased by 16%, 17%, and 16% respectively by using the Spearman correlation coefficient to extract the electrical feature quantities. The values of accuracy, F-measure, and AUC of comparison method 2 are increased by 24%, 39%, and 39% respectively. The values of accuracy, F-measure, and AUC of comparison method 3 are all increased by 14%. In particular, the values of accuracy, F-measure, and AUC obtained by the proposed islanding detection method are all increased from .99 to 1, which realizes the error-free detection of the islanding state. This is because after using the Spearman correlation coefficient for feature extraction, features weakly correlated with the MG state are eliminated, and key features with a strong correlation in the process of islanding detection are retained. Feature extraction reduces the errors caused by electrical feature quantities with weak correlation in the process of islanding detection, weakens the over-fitting phenomenon, and improves the accuracy of the islanding detection method.

By analyzing the performance of different detection methods after feature extraction, it can be seen that the values of accuracy and AUC obtained by the proposed method are 9%, 10%, and 2% higher than that obtained by comparison method 1, 2, and 3, respectively. The F-measure of the proposed islanding detection method is 8%, 9%, and 2% higher than that obtained by comparison methods 1, 2, and 3, respectively. This is because islanding detection is a complex process involving a variety of electrical feature quantities. KNN, SVM, and ANN have limited ability to fit and judge the complex electrical variables at the PCC in the islanding MG, and cannot fully learn the correlation between the MG operation states and the electrical feature quantities. The proposed islanding detection method is based on the integrated learner, which can

give full play to the advantages of weak learners in the diversity of structure and parameters, and can fully mine the rules contained in complex electrical feature quantities in data training. Therefore, compared to comparison methods 1, 2, and 3, the proposed islanding detection method has higher detection accuracy and performance.

4.4 Case 2: Comparative analysis of different islanding detection methods in four scenarios

To further verify the performance reliability and superiority of the proposed islanding detection method, all samples in islanding events and grid-connected interference events are combined into a new sample set A, and all samples in islanding events and line fault events are combined into a new sample set B in this case. In addition, all samples in islanding events, grid connection interference events, and line fault events are divided into sample set C and sample set D by stratified proportional sampling method in the ratio of .5:.5. The proposed method, the comparison method 1, 2, and 3 are trained based on sample sets A, B, C, and D, respectively. The accuracy rate accuracy, F-measure, and AUC values of the proposed islanding detection method, comparison methods 1, 2, and 3 are tested. In this case, four scenarios are set as follows:

Scenario 1: According to the ratio of .6:.4, sample set A is divided into a training set and validation set by the stratified proportional sampling method to verify the performance of different islanding detection methods under grid-connected interference.

Scenario 2: According to the ratio of .6:.4, sample set B is divided into a training set and validation set by the stratified proportional sampling method to verify the performance of different islanding detection methods under grid-connected interference.

Scenario 3: The proposed islanding detection method, the comparison method 1, 2, and 3 are trained by sample set C. Sample set D is used as the verification set to test the islanding detection methods trained by sample set C.

Scenario 4: The proposed islanding detection method, comparison methods 1, 2, and 3 are trained by sample set D. Sample set C is used as the verification set to test the islanding detection methods trained by sample set D.

The accuracy values of the proposed islanding detection method, comparison methods 1, 2, and 3 in four scenarios are shown in Figure 8, the F-measure is shown in Figure 9, and the AUC values are shown in Figure 10. From Figures 8–10, it can be seen that in the verification of the four test scenarios, the proposed method is significantly better than the comparison methods 1, 2, and 3 in the three evaluation indicators of accuracy, F-measure, and AUC values on the validation samples. In scenario 1, the accuracy and AUC values obtained by the proposed islanding detection method are 10%, 7%, and 3% higher than those of comparison methods 1, 2, and 3, respectively. The F-measure value obtained by the proposed islanding detection method are 10%, 7%, and 4% higher than those of comparison methods 1, 2, and 3, respectively. In scenario 2, the accuracy and F-measure values obtained by the proposed islanding detection method are 1% higher than those of comparisons 1, 2, and 3. The AUC value obtained by the proposed islanding detection method are 1%, 2%, and 2% higher than those of comparison methods 1, 2, and 3, respectively. The data shows that compared with comparison methods 1, 2, and 3, the proposed islanding detection method

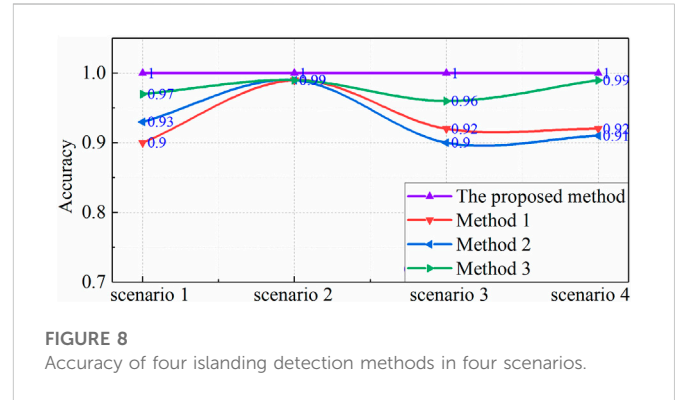


FIGURE 8 Accuracy of four islanding detection methods in four scenarios.

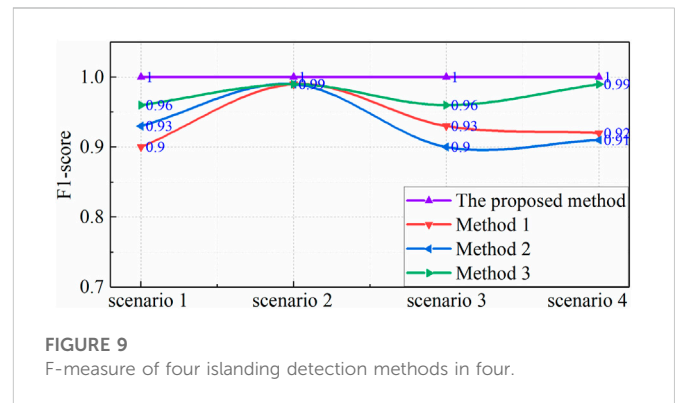


FIGURE 9 F-measure of four islanding detection methods in four scenarios.

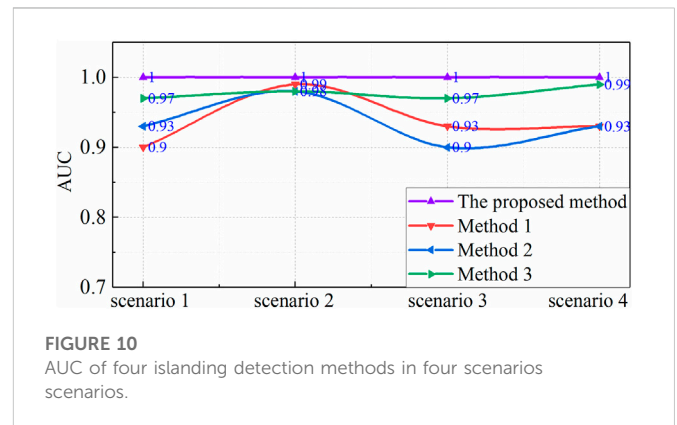


FIGURE 10 AUC of four islanding detection methods in four scenarios.

has a higher detection accuracy in the presence of grid-connected interference and line faults.

In the cross-validation of scenario 3 and scenario 4, with the increase in the complexity of the composition of the test samples, the three evaluation indexes of accuracy, F-measure, and AUC values obtained by comparison methods 1, 2, and 3 fluctuated greatly, and the values ranged from .9 to .99. On the contrary, the proposed islanding detection method is relatively stable in the three evaluation indexes of accuracy, F-measure, and AUC values, and the values all reach 1. This data shows that the proposed islanding detection method can detect islanding more accurately for complex verification samples in the presence of grid

connection interference and line fault. In four different scenarios, the proposed islanding detection method can accurately detect islanding and non-islanding states. In addition, compared with the comparison methods 1, 2, and 3, the proposed islanding detection method can better detect islanding correctly under different sample compositions. They have a large leading amplitude, which fully shows that compared with the traditional single machine learning algorithm, the proposed islanding detection method gives full play to the advantages of the integrated learner in the multidimensional data processing. The data set can be fully learned to determine the threshold value of electrical feature quantities in the process of islanding detection and has higher detection accuracy.

5 Conclusion

To determine the threshold value of various electrical feature quantities, reduce the dead zone in the process of islanding detection, and then realize the accurate detection of islanding, an islanding detection method based on CatBoost is proposed. The method realizes the accurate islanding detection of the MGs by deep excavating the electrical feature quantities at the PCC. Compared with existing methods, the proposed islanding detection method has the following advantages:

- 1) The proposed islanding detection method uses the Spearman correlation coefficient to extract the features of the electrical feature quantities at the PCC, reducing the error caused by the electrical feature quantities with weak correlation in the islanding detection process.
- 2) The proposed islanding detection method can more accurately determine the threshold of electrical feature quantities and reduce the dead zone of islanding detection.
- 3) The proposed islanding detection method can avoid the interference caused by grid-connected interference and line faults, and has higher islanding detection accuracy.

References

- Alshareef, S., Alshareef, S., and Alshareef, W. G. (2014). A new approach based on wavelet design and machine learning for islanding detection of distributed generation. *IEEE Trans. Smart Grid* 5, 1575–1583. doi:10.1109/tsg.2013.2296598
- Baghaee, H. R., Baghaee, D., Nikolovski, S., and Dragicević, T. (2020). Support vector machine-based islanding and grid fault detection in active distribution networks. *IEEE Trans. Emerg. Sel. Top. Power Electron* 8, 2385–2403. doi:10.1109/jestpe.2019.2916621
- Bakhshi, M., Noroozian, R., and Gharehpetian, G. B. (2018). Novel islanding detection method for multiple DGs based on forced Helmholtz oscillator. *IEEE Trans. Smart Grid* 9, 6448–6460. doi:10.1109/tsg.2017.2712768
- Bakhshi-Jafarabadi, R., Sadeh, J., Sadeh, J. d. J., and Popov, M. (2021). Two-level islanding detection method for grid-connected photovoltaic system-based microgrid with small non-detection zone. *IEEE Trans. Smart Grid* 12, 1063–1072. doi:10.1109/tsg.2020.3035126
- Chaitanya, B. K., Yadav, A., and Pazoki, M. (2021). Reliable islanding detection scheme for distributed generation based on pattern-recognition. *IEEE Trans. Ind. Inf.* 17, 5230–5238. doi:10.1109/tii.2020.3029675
- Davari, M., Gao, W., Jiang, Z. -P., and Lewis, F. L. (2021). An optimal primary frequency control based on adaptive dynamic programming for islanded modernized microgrids. *IEEE Trans. Autom. Sci. Eng.* 18, 1109–1121. doi:10.1109/tase.2020.2996160
- Ezzat, A., Ezzat, B. E., and Abdelsalam, A. A. (2021). Microgrids islanding detection using Fourier transform and machine learning algorithm. *Electr. Power Syst. Res.* 196, 107224. doi:10.1016/j.epsr.2021.107224
- Faqhruldin, O. N., El-Saadany, E. F., and Zeineldin, H. H. (2014). A universal islanding detection technique for distributed generation using pattern recognition. *IEEE Trans. Smart Grid* 5, 1985–1992. doi:10.1109/tsg.2014.2302439
- Gupta, P., Bhatia, R. S., and Jain, D. K. (2015). Average absolute frequency deviation value based active islanding detection technique. *IEEE Trans. Smart Grid* 6, 26–35. doi:10.1109/tsg.2014.2337751
- Jia, K., Yang, Z., Zheng, L., Zhu, Z., and Bi, T. (2021). Spearman correlation-based pilot protection for transmission line connected to PMSGs and DFIGs. *IEEE Trans. Ind. Inf.* 17, 4532–4544. doi:10.1109/tii.2020.3018499
- Kermany, S. D., Kermany, M., Deilami, S., and Masoum, M. A. S. (2017). Hybrid islanding detection in microgrid with multiple connection points to smart grids using fuzzy-neural network. *IEEE Trans. Power Syst.* 32, 2640–2651. doi:10.1109/tpwrs.2016.2617344
- Liu, C., Wang, W., Wang, Z., Chen, S., Su, P., Gao, H., et al. (2022). Optimal operation and locating method of new energy building with shared charging service. *Front. Energy Res.* 10, 865060. doi:10.3389/fenrg.2022.865060
- Makwana, Y. M., and Bhalja, B. R. (2019). Experimental performance of an islanding detection scheme based on modal components. *IEEE Trans. Smart Grid* 10, 1025–1035. doi:10.1109/tsg.2017.2757599
- Mlakić, D., Baghaee, H. R., and Nikolovski, S. (2019). Gibbs phenomenon-based hybrid islanding detection strategy for VSC-based microgrids using frequency shift, $\$THD_{[U]\$}$, and $\$RMS_{[U]\$}$. *IEEE Trans. Smart Grid* 10, 5479–5491. doi:10.1109/tsg.2018.2883595

Data availability statement

The raw data supporting the conclusion of this article will be made available by the authors, without undue reservation.

Author contributions

RC, LZ, CX, HX, and ZZ performed the main data analysis and wrote the paper. XH and QD supervised the research activities and reviewed the paper. CW contributed to the discussion. All authors reviewed the manuscript.

Funding

This work was supported by the Science and Technology Program of State Grid Hubei Electric Power Co., Ltd. under Grant B31538221024.

Conflict of interest

The authors declare that this study received funding from the Science and Technology Program of State Grid Hubei Electric Power Co., Ltd. The funder had the following involvement in the study: design, collection, analysis, interpretation of data, the writing of this article, and the decision to submit it for publication.

Publisher's note

All claims expressed in this article are solely those of the authors and do not necessarily represent those of their affiliated organizations, or those of the publisher, the editors and the reviewers. Any product that may be evaluated in this article, or claim that may be made by its manufacturer, is not guaranteed or endorsed by the publisher.

- Murugesan, S., Murali, V., and Daniel, S. A. (2018). Hybrid analyzing technique for active islanding detection based on α -Axis current injection. *IEEE Syst. J.* 12, 3608–3617. doi:10.1109/jsyst.2017.2730364
- Özcanlı, A. K., and Özcanlı, M. (2022). A novel Multi-LSTM based deep learning method for islanding detection in the microgrid. *Electr. Power Syst. Res.* 202, 107574. doi:10.1016/j.epr.2021.107574
- Samat, A., Li, E., Du, P., Liu, S., Miao, Z., and Zhang, W. (2022). CatBoost for RS image classification with pseudo label support from neighbor patches-based clustering. *IEEE Geosci. Remote. Sens. Lett.* 19, 1–5. doi:10.1109/lgrs.2020.3038771
- Samat, A., Li, E., Du, P., Liu, S., and Xia, J. (2021). GPU-accelerated CatBoost-forest for hyperspectral image classification via parallelized mRMR ensemble subspace feature selection. *IEEE J. Sel. Top. Appl. Earth Obs. Remote Sens.* 14, 3200–3214. doi:10.1109/jstars.2021.3063507
- Seyedi, M., Taher, S. A., Ganji, B., and Guerrero, J. (2021). A hybrid islanding detection method based on the rates of changes in voltage and active power for the multi-inverter systems. *IEEE Trans. Smart Grid* 12, 2800–2811. doi:10.1109/tsg.2021.3061567
- Sivadas, D., and Vasudevan, K. (2020). An active islanding detection strategy with zero nondetection zone for operation in single and multiple inverter mode using GPS synchronized pattern. *IEEE Trans. Ind. Inf.* 67, 5554–5564. doi:10.1109/tie.2019.2931231
- Wang, C., Chu, S., Ying, Y., Wang, A., Chen, R., Xu, H., et al. (2022). Underfrequency load shedding scheme for islanded microgrids considering objective and subjective weight of loads. *IEEE Trans. Smart Grid*, 1. doi:10.1109/TSG.2022.3203172
- Wang, C., Chu, S., Yu, H., Ying, Y., and Chen, R. (2022). Control strategy of unintentional islanding transition with high adaptability for three/single-phase hybrid multimicrogrids. *Int. J. Electr. Power Energy Syst.* 136, 107724. doi:10.1016/j.ijepes.2021.107724
- Wen, B., Boroyevich, D., Burgos, R., Shen, Z., and Mattavelli, P. (2016). Impedance-based analysis of active frequency drift islanding detection for grid-tied inverter system. *IEEE Trans. Ind. Appl.* 52, 332–341. doi:10.1109/tia.2015.2480847
- Xia, X., Xiao, Y., Liang, W., and Cui, J. (2022). Detection methods in smart meters for electricity thefts: A survey. *Proc. IEEE Inst. Electr. Electron Eng.* 110, 273–319. doi:10.1109/jproc.2021.3139754
- Zhang, R., Li, G., Bu, S., Kuang, G., He, W., Zhu, Y., et al. (2022). A hybrid deep learning model with error correction for photovoltaic power forecasting. *Front. Energy Res.* 10, 948308. doi:10.3389/fenrg.2022.948308
- Zhang, W., Wei, Z., Wang, B., and Han, X. (2016). Measuring mixing patterns in complex networks by Spearman rank correlation coefficient. *Phys. A* 451, 440–450. doi:10.1016/j.physa.2016.01.056
- Zhao, G., Ding, W., Tian, J., Liu, J., Gu, Y., Shi, S., et al. (2022). Spearman rank correlations analysis of the elemental, mineral concentrations, and mechanical parameters of the lower cambrian niutitang shale: A case study in the fenggang block, northeast guizhou Province, south China. *J. Pet. Sci. Eng.* 208, 109550. doi:10.1016/j.petrol.2021.109550